CZECH TECHNICAL UNIVERSITY IN PRAGUE

FACULTY OF MECHANICAL ENGINEERING

DOCTORAL THESIS STATEMENT

Czech Technical University in Prague
Faculty of Mechanical Engineering

Department of Mechanics, Biomechanics
and Mechatronics

Summary of Dissertation

Clinical Biomechanics of Hip Joint

Ing. Jana Hornová

Doctoral study programme: Mechanical Engineering

Field of study: Biomechanics

Advisor: Prof. RNDr. Matej Daniel, Ph.D.

2017 Prague

Title in Czech: Klinická biomechanika kyčelního kloubu

A dissertation submitted to the Department of Mechanics, Biomechanics and Mechatronics, Faculty of Mechanical Engineering, Czech Technical University in Prague in partial fulfillment of the requirements for the degree of doctor of philosophy.

Author:	Ing. Jana Hornová Department of Mechanics, Biomechanics and Mechatronics, Faculty of Mechanical Engineering, CTU in Prague Technická 4, 166 07, Prague, Czech Republic
Advisor:	Prof. RNDr. Matej Daniel, Ph.D. Department of Mechanics, Biomechanics and Mechatronics, Faculty of Mechanical Engineering, CTU in Prague Technická 4, 166 07, Prague, Czech Republic
Opponents:	prof. MUDr. David Pokorný, CSc. doc. Ing. Zdeněk Horák, Ph.D. doc. Ing. Patrik Kutílek, Ph.D.

Summary of dissertation was distributed on .....

Thesis defence will be held on ..... at ..... at seminar room 17 (ground floor), Faculty of Mechanical Engineering, CTU in Prague, Technická 4, 166 07, Prague.

Full version of thesis is available at Department for Science and Research, Faculty of Mechanical Engineering, Technická 4, 166 07, Prague.

Prof. RNDr. Matej Daniel, Ph.D.
Chairman of Comittee of the field of Biomechanics
Faculty of Mechanical Engineering, CTU in Prague

Annotation

Multiple assumptions about model's geometry, mechanical properties and physiological parameters are adopted when using biomechanical models in clinical studies. The aim of this thesis is to assess how a patient-specific hip joint modelling could affect prediction of biomechanical parameters. The studied parameters ranged from geometrical parameters through hip joint reaction forces prediction to joint contact stress estimation. It was shown that the input geometrical parameters obtained from planar radiographs are influenced by the patient's obesity and X-ray device considerably. The musculoskeletal model of hip joint loading was validated against experimental data for a single patient. However, scaling the musculoskeletal model to individual patients by a standard procedure based on single pelvic bone dimension underestimates the range of hip joint reaction force. It was shown that change in individual muscle capacity to generate the force influences the hip muscle force distribution but not the hip joint reaction force. Simple model of hip contact geometry could predict the overall stress distribution but not the absolute values of contact stress peaks. To conclude, patient specific modelling could provide more reliable results for given patients if accurate input parameters and scaling procedures are adopted correctly. When considering limitations of generic models described in this study, these models could be used to predict general trends in clinical studies.

Anotace

Pro použití biomechanických modelů v klinických studiích jsou přijímány zjednodušující předpoklady o geometrii daného modelu, jeho mechanických vlastnostech a fyziologických parametrech. Cílem této disertační práce je stanovit, jak jsou biomechanické parametry ovlivněny, je-li matematický model kyčelního kloubu přizpůsoben na míru danému pacientovi. V klinických studiích byly zkoumány geometrické parametry, určeny reakční síly v kyčelním kloubu a kontaktní tlaky v kloubu jak ve zjednodušených modelech, tak i v modelech upravených podle konkrétního pacienta. V rámci této práce bylo ukázáno, že rozměry odečtené z rentgenových snímků jsou značně ovlivněny použitým RTG přístrojem i obezitou pacienta. Nesprávně určené rozměry kostí pacienta vedou k nepřesnostem v určení reakční síly v kyčelním kloubu. Další chyba ve stanovení reakční síly může být vnesena zjednodušeným škálováním obecného svalově-kosterního modelu. Správně určená velikost a směr reakční síly a přesná geometrie kyčelního kloubu jsou důležité pro určení velikosti kontaktního tlaku. Zjednodušený model kyčelního kloubu dokáže předpovídat celkové rozložení kontaktního tlaku v kyčelním kloubu, nicméně nedokáže předpovědět jeho lokální maxima. Na závěr lze říci, že jsou-li použity přesné vstupní parametry a model je správně naškálován, tak modelováním uzpůsobeným na míru daného pacienta je možné dosáhnout spolehlivějších výsledků. Pomocí zjednodušeného modelu je možné předpovídat celkové trendy biomechanických parametrů v rámci klinických studií, jsou-li respektována jednotlivá omezení modelu.

Acknowledgement

I would like to thank to prof. RNDr. Matej Daniel, Ph.D. for his unshakeable faith in this topic which helped me to continue and find subsequent way between blind alleys and for last year full of very intensive collaboration.

I would like to express gratitude to my colleagues dr. Martin Nesládek, Ing. Viktor Kulíšek, dr. Jan Papuga, dr. Jakub Jura, dr. Petr Tichý, ing. Tereza Voňavková, Ing. Ján Kužma, Ing. Katarina Mendová, dr. Jakub Kronek, dr. Tomáš Goldmann and dr. Miloslav Vilímek and former colleagues dr. David Hromádka, Ing. Jan Veselý and dr. Tomáš Bouda for inspiring discussions, help with inter-observer variability study, useful advices and mainly for the support and encouragement.

Next, words of thanks belong to my former boss dr. Matěj Sulitka and actual boss Ing. Jindřich Kubák for their patience with my time demands, words of encouragement and fantastic cooperation.

Last of all I would like thank to my family and my friends. Especially my grandmas motived me to finish this doctoral thesis. Their curious questions "how" and "why" forced me to think about problems differently and their questions "when" were insistent. Thank you for that. My parents were with me all long years of my studies and thesis writing, sometimes with small doubts but they have believed in me. Thank you too. I can not imagine to finish my thesis without my friends, my thanks belongs especially to Ing. Petr Němeček, Miroslava Nováková, Ing. Robert Halama, Matěj Morava, MD Karel Štěpánek, Jan Fleišmann and my cousin Ing. Zuzana Brodská.

Contents

CHAPTER 1

Introduction

Musculoskeletal models are used to predict muscle and joint reaction forces in order to analyse complex biomechanical problems, such as the functional outcome after surgery [42]. Furthermore, musculoskeletal models have been used to model the effects of a stroke [26], spinal cord injuries [40] and sport injuries [33].

The biomechanical modelling have mostly been used to understand mechanical principles of the human body. The qualitative rather than quantitative informations were obtained and the model were frequently built on data from various cadaveric studies. These models, although built on data of specific patients, are more interested in trends that can be reliably predicted across a population.

Patient-specific modeling is the development of computational models of human pathophysiology that are individualized to patient-specific data [38]. Patient-specific biomechanical modelling is gaining more attention because of its potential to improve diagnosis, optimize clinical treatment by predicting outcomes of therapies and surgical interventions, and design of surgical training platforms.

Most current medical diagnostic practices lead to rough estimates of outcomes for a particular treatment plan, and treatments and their outcomes usually find their basis in the results of clinical trials. However, these results might not apply directly to individual patients because they are based on averages [38]. Although largely unexplored, biomechanical models have potential of investigating predictive if-then scenarios such as post-operative functional outcomes after virtual interventions in individual patients [24]. The efficacy of computational models to predict whether or not a medical intervention will be successful often depends on subtle factors operating at the level of unique individuals.

However, the ability to predict such behaviour is hampered by significant levels of variability that are present in all aspects of human biomechanics, including dimensions and material properties

[51], stature [17], function [48], and pathological conditions [22]. In addition to variability between the patients, the models adopt multiple assumptions and estimation regarding definition of body segments dimensions and inertial properties [16], muscle action physiology [10], prediction of muscle, tendon and joint forces [29] or constitutive equations of soft and hard tissue [52].

With current imaging modalities, a geometry of a tissue or organ is relatively easy to obtain. Assigning material properties to these geometries is more uncertain. Theoretically, we may create a patient-specific musculoskeletal model for each patient if medical image data are available. However, whole-body CT (computed tomography) or MRI (magnetic resonance imaging) scans are time-demanding and CT presents a high radiation exposure for patients. Even, if these data would be available, Correa et al., 2011 reported that processing time of single MRI-based model exceeds 10 hours, with the majority of this time insensitive to computing power [14].

An alternative to create patient-specific model is adaptation of generic models to given patient. Scaled-generic models are created by scaling body-segment anthropometry, joint geometry, and muscle-tendon attachment sites in the model to corresponding parameters in individual subjects. Such scaling requires measurements of patients geometry often estimated on basis of few characteristic dimensions. The accuracy of scaling methods in generic models remains largely untested. Therefore we would like to address relationship between accuracy of input data and methods to the results of musculoskeletal models. To deal with the variability of all parameters representing musculoskeletal model is out of the scope of this thesis. Therefore we focus on methods of scaling geometrical parameters and on methods how these parameters are obtained. The main source of data within our studies are anteroposterior (AP) radiographs, as these are available in clinical archives and present a radiographic exams are typically performed in clinics for most of the patients.

The object of the study is the hip joint. Hip joint is one of the largest joints in the body with relatively simple ball and joint geometry. Many biomechanical studies on hip joints and their replacements require detailed knowledge of the loads acting in this joint. Therefore multiple methods have been developed to study hip joint load and hip joint contact stress distribution. The thesis shows applicability of selected method in the patient-sepcific analysis of the hip joint.

CHAPTER 2

Aims

The complexity of current patient-specific models is a reason of their rare used in the clinical practice. Therefore, multiple assumptions about model's geometry, mechanical properties and physiological parameters are adopted when using biomechanical models in clinical studies. Within the current study, we would like to specify how the assumptions used in model constructions influence their results. The principal aim of this thesis is to assess how a patient-specific hip joint modelling affects prediction of biomechanical parameters in comparison to generic models.

The specific aims of the thesis are:

1. Verify hypothesis that the magnification of radiographs depends on the workplace where it is taken.

2. Test the hypothesis that obesity type affects hip radiographic magnification and quantify the relationship between patient body habitus and radiographic magnification.

3. Quantify the effect of isotropic and anisotropic scaling on the hip joint reaction force assessment.

4. Validate the generic musculoskeletal model of the lower limb by comparison of predicted hip joint reaction force to experimental data.

5. Determine the effect of maximum isometric force change in individual muscle and muscle group to hip muscle force and to hip joint reaction force prediction.

6. Determine the effect of patient-specific hip joint geometry on hip contact stress distribution.

CHAPTER 3

Methods

3.1 Hip imaging – body measurements for scaling

It is essential to know accurate dimension of bone geometry for biomechanical analysis. The radiographic images are mostly used to determine bone dimensions however, they are subjected to errors in dimensions and shapes. Magnitude of errors are influenced by various factors: e.g. X-ray machine construction (mutual distances between photosensitive plate–table–X-ray source), horizontal shift from the centre of an X-ray beam, and patients' body habitus and position, namely the distance between an object and a table (Figure 3.1). Accurate knowledge of the radiographic magnification is fundamental for orthopaedic surgeons when planning the surgery, e.g. total hip arthroplasty. Accurate planning can reduce postoperative complications and help to preserve hip joint biomechanics. This clinical study was aimed to determine the influence of different X-ray machine (radiological workplace) and patients' body habitus on the radiographic magnification.

3.1.1 Influence of workplace

The dataset included 337 AP radiographs (Table 3.1) gathered at five orthopaedic departments and five different radiological devices in the Czech Republic.

3.1.2 Influence of obesity

The study included 303 patients, 125 male and 178 female.

The radiographic magnification M differs at each clinic because of different radiological equipment and image handling. To compare

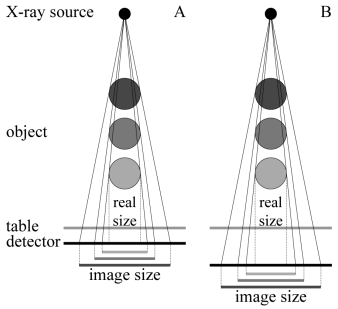

(a) A and B are various positions of hip joint over the table, (A vs. B) various radiological setups [57].

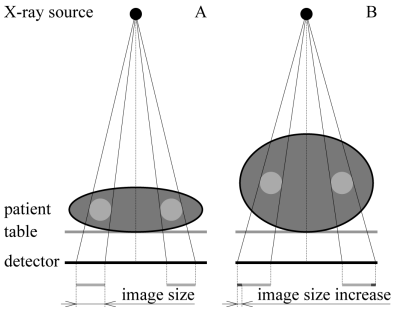

(b) Radiographic magnification in A a normal and B an obese patient. Owing to the higher position of the hip above the table in the obese patient B, the image size of the femoral head is larger than in a normal patient A [58].

Figure 3.1: Schematic diagram showing radiological magnification.

Table 3.1: Clinics and patients included in the study [57].

	Institution	Total	Male	Female
A	Department of Radiology, Hospital Jablonec nad Nisou	52	22	30
B	Department of Orthopaedics, Second Faculty of Medicine, Charles University in Prague and Teaching Hospital Motol	59	23	36
C	Department of Orthopaedics, Hospital in Pelhřimov	108	44	64
D	Department of Orthopaedics, First Faculty of Medicine, Charles University in Prague and Teaching Hospital Motol	43	20	23
E	Department of Orthopaedics, Faculty of Medicine and Dentistry, Teaching Hospital, Palacký University Olomouc	75	24	51

the global effect of obesity on change in radiographic magnification, the data from each clinic were normalized relative to zero median. Difference from median (ΔM) was used in further analysis. Analysis of original data for each clinic is provided as well.

3.2 Influence of scaling to the reaction force

The knowledge of hip joint reaction force is important for understanding joint injuries, diseases development, and accurate testing and development of hip joint implants. Nowadays, the hip joint reaction force is calculated from musculoskeletal models which are rarely adjusted to particular patient. The generic musculoskeletal model is scaled just by one or two parameters mostly. This section is focused on the influence of scaling method to the variability and magnitude of hip joint reaction force.

3.2.1 Patient-specific data

250 radiograms of adult human hips were obtained from the archive of the Department of Orthopaedic Surgery and the Department of Traumatology, Ljubljana University Medical Centre, Ljubljana, Slovenia. 356 hips were included in the study.

The hip joint center (HJC) was chosen at the center of the circle fitting the bony surface of the femoral head. The geometry of an individual hip was described by the following parameters (Figure 3.2): interhip separation l (the distance between the left and right HJC), iliac height H (the vertical distance between the most superior point on the ilium and HJC), iliac width C (the horizontal distance between the most lateral point on the ilium and HJC) and the coordinates of the effective muscle insertion point on the greater trochanter in the femoral coordinate system (T_y and T_z, respectively).

3.2.2 Scaled musculoskeletal model

Reference musculoskeletal model was scaled to individual one using patient-specific data from anteroposterior radiograms. Three types of model scaling were defined, Figure 3.2: Type A – anisotropic scaling, the pelvis and femur are scaled separately and anisotropically. Type B – isotropic scaling, the distances are scaled by pelvic width $W = l + 2 \cdot C$. Type C – isotropic scaling, the distances are scaled by the interhip separation l.

One-legged stance representing midstance phase of walking is taken as a representative body position for hip joint force calcula-

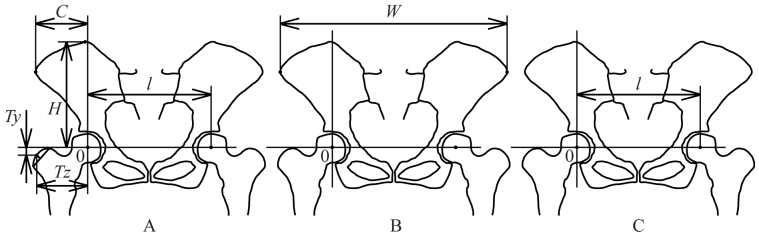

Figure 3.2: Scaling methods: A – anisotropic scaling by: interhip separation l, height of the ilium H, width of the ilium C and inferior and lateral position of grater trochanter T_y and T_z , respectively. B — isotropic scaling by the width of the pelvis $W = l + 2 \cdot C$ and C – isotropic scaling by the interhip separation l [56].

tion, Figure 3.3. Complete process of hip joint force estimation is demonstrated in Figure 3.3. The hip joint reaction force is calculated relative to the body weight $\mathbf{F_R}/\mathbf{BW}$.

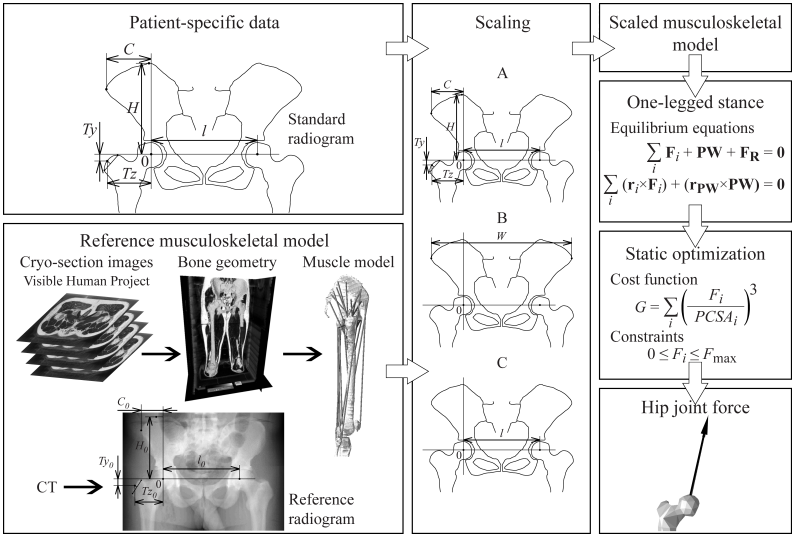

Figure 3.3: Hip joint force estimation workflow with three different scaling methods [63]. Equlibrium equations are defined in Iglič et al., 2002 [28].

3.3 Validation of calculated hip joint reaction force to in vivo measurements

The basic method of model verification is comparison to the experimental data. In this study, the hip joint reaction force was calculated by musculoskeletal model using inverse dynamic optimization. Data from telemetric hip prosthesis of Bergmann et al., 2001 [7] are taken as a gold standard of experimental estimation of hip joint reaction force. So, the calculated results were compared to these data, the influence of scaling to the hip joint reaction force was study.

3.4 Contribution of musculoskeletal model characteristics to hip muscle and force prediction

In addition to the bone geometry variability described above, an interpatient variability in muscle parameters can be observed. Namely, a physiological cross-sectional area of the muscle $PCSA$, maximal isometric force $F_{\max}$, pennetation angle Θ can be given as examples. The musculoskeletal models usually scale muscle origin and insertion together with bone geometry but parameters mentioned above stay fixed. The aim of this study was to show how a change of maximal isometric force $F_{\max}$ of a separate muscle or separate muscle group affects a magnitude of hip joint reaction force and muscle force distribution.

The muscle activation and joint loading was estimated using OpenSim software [19] (version 3.1, Standford USA). Within this study, a generic muscle model with 23 degree of freedom and 92 muscle-tendon actuators was adopted [20], (Figure 3.4). Following muscle-tendon actuators were evaluated: m. gluteus maximus (1 segment, glut max), m. gluteus medius (3 segments, glut med 1-3), m. gluteus minimus (3 segments, glut min 1-3), m. piriformis (piri), m. sartorius (sar) and m. tensor fascie latae (tfl).

The maximum force during the walking cycle in normal gait is reported in the first segment of gluteus medius (glut med 1) and this muscle actuator was chosen for local strengthening. Muscle strengthening was imposed by two ways. First, the maximum isometric force in single muscle-tendon actuator (glut med 1) was dou-

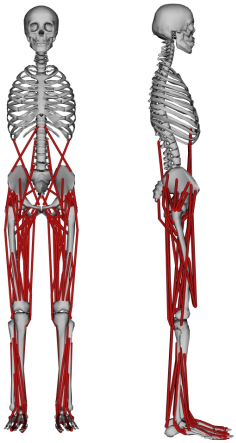

(a) (b)

Figure 3.4: Generic muscle model, 92 muscle-tendon actuators [20], (a) Anterior, (b) Lateral.

bled to study the effect of localized strengthening. Second, all muscle actuators corresponding to principal muscle abductors gluteus medius and minimus (6 actuators) were strengthened by doubling their respective maximum isometric force.

3.5 Contact stress calculation

Beside the hip joint reaction force estimation, the contact stress distribution may predict the joint development. The knowledge of contact stress distribution could be used to identify potentially risky hips and predict their prospective treatment. Together with loading force, the knowledge of weight-bearing area geometry is needed to calculate hip stress. The aim of this part is to determine how the patient-specific geometry of weight-bearing areas affects the estimation of contact stress distribution.

3.5.1 Geometry

For hip contact stress distribution determination, the geometric model of cartilage was required. Two approaches were considered.

Firstly a semiautomatic segmentation where borders of cartilage should be detected by a computer algorithm. The first step for semiautomatic edge detection was the determination of image region where the whole hip joint cartilage is displayed Figure 3.5. All image processing was scripted in Matlab ver. R2009b, The MathWroks Inc., USA [34] and GUI was created. Secondly a manual segmentation where border of bone should be identified manually.

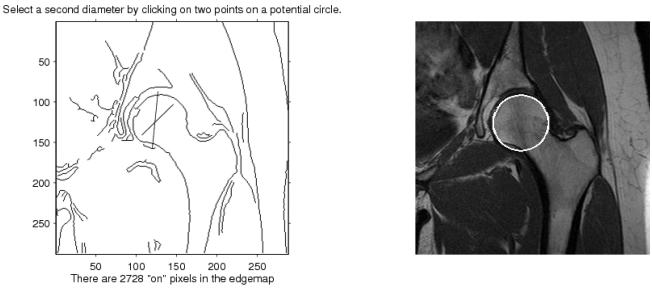

(a) (b)

Figure 3.5: GUI: (a) After edges detection, two diameters of demanded circle are selected. (b) 1 circle is detected. Circle detected at center (130 126) with radius 34, represented in the original DICOM image.

Patients' data

Two patient-specific models based on CT and MRI images were created within this study. The boundary of bones (femur and pelvis) were manually segmented from (a) transversal CT images of a female cadaver of the Visible Human Project [3]; (b) in vivo taken MRI male images. The Delaunay triangulation [1, 43] was done in angular spherical coordinates, Figure 3.6.

3.5.2 Numerical model

Mathematical model assumptions

Mathematical model for contact stress calculation was derived within this study. Following assumptions were taken into account to simplify the problem.

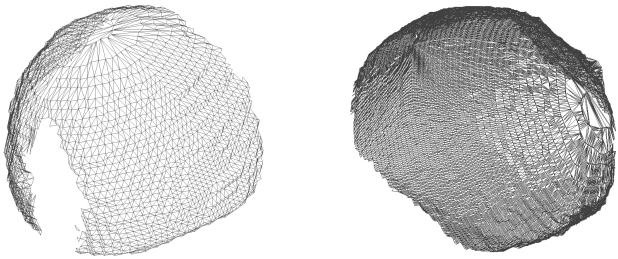

(a) Triangulation based on CT images.

(b) Triangulation based on MRI images.

Figure 3.6: 3D triangulation of femoral head surface [61].

- The space between acetabulum and femoral head is filled by cartilage. The places where a cartilage thickness is higher than 4 mm were excluded from the model, because they were not physiological. From anatomical point of view it may correspond to region of a ligament or fossa acetabuli.
- Smooth, well lubricated surfaces with negligible friction are considered, i.e. normal stresses are acting at the cartilage surface.
- Cartilage was considered to be linearly elastic [13].

Contact stress model formulation

General contact stress model was formulated as follows. Let $\mathbf{F_R}$ be a known resultant hip reaction force, i.e. a loading force within this model. Let a surface of weight bearing area of femoral head A be divided into the triangular elements. Each element A_i transfers a force $\mathbf{F_{R}}_i$ (Eq. 3.1), where n is a number of elements and i is an index of element. It follows that

$$\mathbf{F_R} = \sum_{i=1}^{n} \mathbf{F_{R}}_i \qquad\qquad A = \sum_{i=1}^{n} A_i. \tag{3.1}$$

The model is depicted on the Figure 3.7. Centre of fitted sphere is denoted as O. T_i is a center of area of element A_i on femoral head surface and $\mathbf{n}_i$ is a normal vector to the element A_i. A_{ti} is a nearest point on an acetabular surface to the T_i in $\mathbf{n}_i$ direction. Since it

is assumed that the space between femoral head and acetabulum is filled by a cartilage, the distance between points T_i and A_{ti} is a cartilage thickness h_i, (Eq. 3.2).

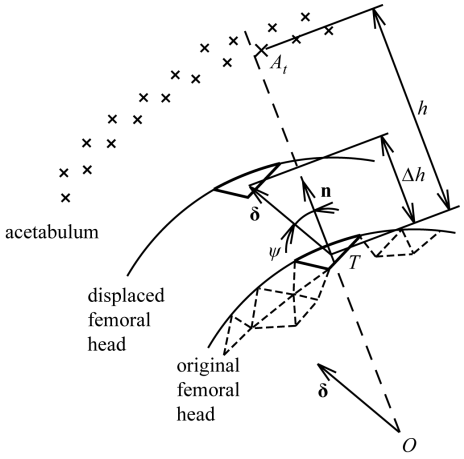

Figure 3.7: Cartilage model scheme.

$$\left|\left(\overrightarrow{T_i A_{ti}}\right)\right| = h_i \qquad \overrightarrow{T_i A_{ti}} = h_i \cdot \mathbf{n}_i \tag{3.2}$$

If the hip joint is loaded by force $\mathbf{F_R}$, the femoral head moves towards an acetabular cup. Let $\boldsymbol{\delta}$ be displacement of femoral head. All points of femoral head area displaced by $\boldsymbol{\delta}$, if femoral head is considered as rigid, Figure 3.7. A change of cartilage thickness Δh is depended on directions of normal vector $\mathbf{n}$ and displacement vector $\boldsymbol{\delta}$ forming an angle ψ. It is apparent (Figure 3.7) that $\cos\psi = \Delta h / |\boldsymbol{\delta}|$ and since the scalar product of vectors equals to product of their magnitudes and cosine of their angle, it follows that

$$\Delta h_i = |\boldsymbol{\delta}| \cdot \cos\psi = |\boldsymbol{\delta}| \cdot \underset{=1}{|\mathbf{n}|} \cdot \cos\psi = \boldsymbol{\delta} \cdot \mathbf{n}. \tag{3.3}$$

The strain ε of cartilage can be expressed

$$\varepsilon_i = \frac{\Delta h_i}{h_i} = \frac{\boldsymbol{\delta} \cdot \mathbf{n}_i}{h_i}. \tag{3.4}$$

Elastic cartilage behaviour is assumed [13], i.e. the Hooke's law $\sigma = \varepsilon \cdot E$ can be expressed $p_i = \varepsilon_i \cdot E$ where the hip joint contact

stress is denoted as p, the strain as ε and Young's modulus as E. The contact stress for each element can be formulated with Eq. 3.4 as follows

$$p_i = \frac{\boldsymbol{\delta} \cdot \mathbf{n}_i}{h_i} \cdot E. \tag{3.5}$$

The contact can bear compressive loading only, i.e. the elements where $\boldsymbol{\delta} \cdot \mathbf{n}_i > 0$ only were considered in further calculations. Let $k = 1, 2, \ldots, N$ where N is a number of elements transmitting pressure.

Let $\mathbf{F_R}(\boldsymbol{\delta})$ be a hip joint reaction force $\mathbf{F_R}$ depending on displacement $\boldsymbol{\delta}$. Using Eq. 3.5, the force can be expressed as

$$\mathbf{F_R}(\boldsymbol{\delta}) = \sum_{k=1}^{N} A_k \cdot \mathbf{p}_k = \sum_{k=1}^{N} A_k \cdot p_k \cdot \mathbf{n}_k \sum_{k=1}^{N} A_k \frac{\boldsymbol{\delta} \cdot \mathbf{n}_k}{h_k} \cdot E \cdot \mathbf{n}_k. \tag{3.6}$$

Eq. 3.6 is nonlinear as the weight-bearing surface A depends on the choice of femoral head displacement $\boldsymbol{\delta}$. The system of equations was solved by Matlab [34] by function *fsolve* [2], the *trust-region dogleg* solving algorithm was used. A solution of this system of equations is a vector of displacement $\boldsymbol{\delta}\,(\delta_x, \delta_y, \delta_z)$. When $\boldsymbol{\delta}$ is known, the contact stress p_k can be obtained from Eq. 3.5 for each element.

3.5.3 Verification model

For numerical model verification the simplified model, for which an analytical solution is possible to obtain after Iglič et al., 2002 [28] was considered.

CHAPTER 4

Results

4.1 Hip imaging – body measurements for scaling

4.1.1 Influence of workplace

The aim of this study was to find out if the geometric data taken from plain antero-posterio hip radiographs from various workplaces are homogenous. Two sources of variation were tested: the first is the variation due to radiographic setup at a given workplace and the second is the variation between those workplaces.

Table 4.1: Radiographic magnification gotten at 5 workplaces [66, 57].

Clinic	Mean ± SD	Range
A	118.6 % ± 1.7 %	(113.8 % — 121.4 %)
B	116.2 % ± 1.8 %	(112.5 % — 122.2 %)
C	119.9 % ± 2.4 %	(113.7 % — 125.8 %)
D	118.5 % ± 2.1 %	(113.5 % — 124.3 %)
E	124.2 % ± 2.2 %	(119.6 % — 130.2 %)

The magnification of external marker measured at clinic A (111.5 % ± 0.5 %) and B (109.9 % ± 0.5 %) exhibits almost constant value with low variation between radiographs measured at the same clinic. It confirms identical radiological setup used for all patients at given workplace. Table 4.1 shows radiographic magnifications obtained at five different workplaces. There is a significant effect of the choice of clinic on radiographic magnification ($F(4,332)=132$, $p \leq 0.001$), Figure 4.1. Post-hoc comparisons indicates significantly different radiographic magnification between all hospitals ($p < 0.002$) except for difference in magnification between clinics A and D ($p = 0.99$).

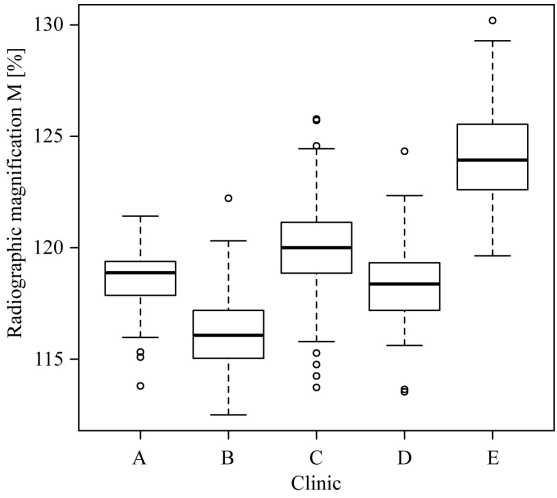

Figure 4.1: Boxplot of radiographic magnification. Hip radiographic magnification measured from radiographs of patients after total hip replacement at five hospitals [66, 57].

4.1.2 Influence of obesity

Patient-specific body parameters influence accuracy of measured biomechanical parameters in addition to radiographic setup. Attention should be paid to patient body habitus, as radiographic magnification should be expected to be higher in obese patients and conversely, less magnification would be expected in thin patients. The aim of this study was to quantify this relationship.

The cohorts from different clinics are comparable in patients' mass, height, BMI, and BSA (t-test, $p \geq 0.2$). Figures 4.3, 4.4, and 4.5 shows dependence between m, BMI, BSA (after Livingston, 2001 [32]) and change in radiographic magnification. Table 4.2 shows correlation coefficients between parameters describing body habitus and radiographic magnification. BSA calculated after Livingston, 2001 [32] exhibits best relationship to radiographic magnification for patients from all hospitals. Therefore this definition of BSA was considered in futher study. The lowest correlation was observed for PI and since PI is mostly not used in clinical practice, the PI was not futher considered. There is obvious difference in magnification between the workplaces. To make aggregate data comparable, radiographic magnification for each workplace was normalized by

median. The change in radiographic magnification ΔM is considered futher. One-way between subject ANOVA was conducted to compare the effect of obesity type on the hip radiographic magnification for patients classified from normal weight to class-II obesity. Obesity has a significant effect on radiographic magnification ($F(3,290)=19.24$, $p < 0.001$). Post-hoc comparison using Tukey's HSD test indicated that the mean change in radiographic magnification is not significantly different between overweight and class-I obese patients ($p = 0.117$, Figure 4.2). The difference between normal weight and overweight patients is on the border of significance ($p = 0.031$, Figure 4.2).

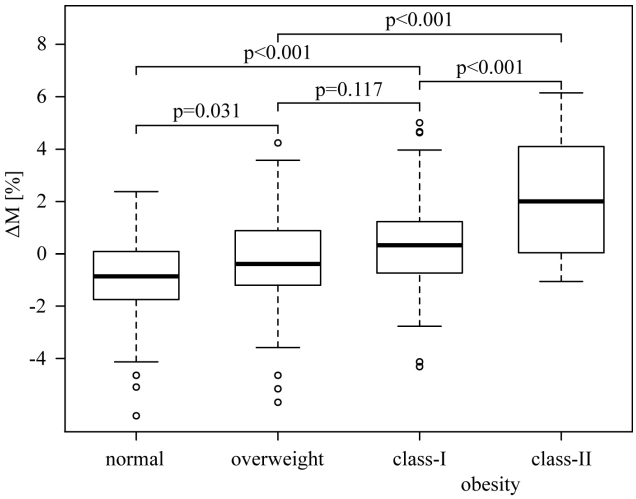

Figure 4.2: Boxplot interaction between hip radiographic magnification and obesity [67, 58]. The vertical axis shows the difference from median magnification determined at each hospital ΔM. The horizontal axis shows the obesity category classified by BMI (p reported from Tukey's post-hoc test).

The higher the mass, BMI or BSA, the higher the radiographic magnification (mass: $r = 0.443$, 95% confidence interval 0.348 – 0.529, BMI: $r = 0.450$, 95% confidence interval 0.355 — 0.535, BSA: $r = 0.443$, 95% confidence interval 0.347 — 0.529). Linear regression analysis demonstrates that for every 17 kg increase in patients' mass (Figure 4.3), 5 kg/m^2 increase in the BMI (Figure 4.4) or for every 0.27 m^2 in the BSA (Figure 4.5) there is a 1 percent increase

in the hip radiographic magnification. Correlation between the patients' mass, BMI, BSA and radiographic magnification is more obvious in females than in males (Tables 4.3 and 4.2), this difference in correlation coefficients is statistically significant (Williams's test p equals 0.008, 0.046, 0.002 for mass, BMI and BSA). 1 percent increase in the hip radiographic magnification corresponds to increase in patients' mass, BMI and BSA for 19 kg, 7 kg/m^2, and 0.29 m^2 in males, respectively and 12 kg, 4 kg/m^2, and 0.19 m^2 in females, respectively.

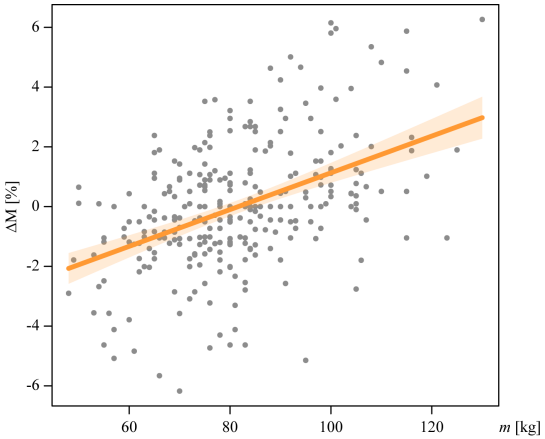

Figure 4.3: The correlation between patients' mass and change in hip radiographic magnification ΔM.

Table 4.2: Comparison of correlation coefficients r for mass (orange), BMI (blue), PI (gray) and BSA (green). Colour denotes statistically significant r (higher then treshold r) at the level $\alpha = 0.05$, $\beta = 0.90$ for given sample sizes. The best r of all BSA methods for each hospital is printed in bold.

Total		$\alpha = 0.05$					BSA			
Number		$\beta = 0.90$	m	BMI	PI	Du Bois	Mosteller	Haycock	Shuter	Livingston	Tikuisis
A	52	0.4310	0.6187	0.5416	0.4322	0.5773	0.6000	0.6080	0.5845	**0.6268**	0.6073
B	59	0.4070	0.4336	0.4257	0.3464	0.3818	0.4064	0.4156	0.3895	**0.4396**	0.4172
C	63	0.3950	0.4088	0.4029	0.3531	0.3623	0.3830	0.3906	0.3688	**0.4095**	0.3817
D	54	0.4240	0.3465	0.4227	0.4217	0.2655	0.2933	0.3048	0.2737	**0.3392**	0.3146
E	75	0.3640	0.5649	0.5649	0.5029	0.4328	0.4727	0.4881	0.4449	**0.5302**	0.4950
Male		$\alpha = 0.05$					BSA			
Number		$\beta = 0.90$	m	BMI	PI	Du Bois	Mosteller	Haycock	Shuter	Livingston	Tikuisis
A	22	0.6260	0.4639	0.2198	0.0842	**0.5548**	0.5307	0.5178	0.5488	0.4667	0.5452
B	23	0.6150	0.3865	0.3224	0.2404	0.3463	0.3680	0.3753	0.3532	**0.3898**	0.3570
C	28	0.5670	0.4004	0.3528	0.3028	0.4104	**0.4119**	0.4114	0.4113	0.4064	**0.4119**
D	28	0.5670	0.2362	0.2186	0.1969	0.2178	0.2240	0.2259	0.2198	**0.2294**	0.2208
E	24	0.6040	0.3018	0.3018	0.2544	0.2450	0.2687	0.2777	0.2523	**0.3017**	0.2567
Female		$\alpha = 0.05$					BSA			
Number		$\beta = 0.90$	m	BMI	PI	Du Bois	Mosteller	Haycock	Shuter	Livingston	Tikuisis
A	30	0.5500	0.6546	0.6033	0.5429	0.5716	0.6107	0.6244	0.5839	**0.6565**	0.6015
B	36	0.5090	0.5540	0.4877	0.4081	0.5406	0.5532	0.5562	0.5452	**0.5577**	0.5509
C	35	0.5150	0.4096	0.4619	0.4599	0.3307	0.3622	0.3741	0.3404	**0.4063**	0.3545
D	26	0.5850	0.7673	0.7013	0.6259	0.7318	0.7422	0.7455	0.7351	**0.7496**	0.7394
E	51	0.4350	0.6299	0.6299	0.5401	0.6979	0.7045	**0.7056**	0.7004	0.7032	0.7033

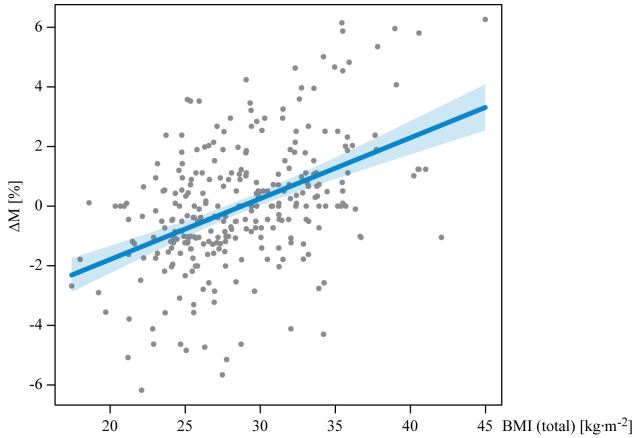

Figure 4.4: The correlation between patients' BMI and change in hip radiographic magnification ΔM [67, 58].

Table 4.3: Pearson correlation coefficient between the patients' parameter and the change in radiographic magnification ΔM [67, 58]. All correlations are statistically significant ($p < 0.001$).

Parameter	Male	Female	Total
m	0.351	0.592	0.443
BMI	0.352	0.539	0.450
BSA (Livingston)	0.300	0.587	0.443

4.2 Influence of scaling to the reaction force

After the patient-specific geometrical parameters are measured either from external measurements or from medical images, the musculoskeletal model is adapted for each patient. Reducing morphological differences between the patient and the model is likely to improve the model accuracy. This study is intended to determine to what extend more accurate scaling will influence prediction of immeasurable hip joint contact forces. Three methods of scaling were tested: (A) anisotropic scaling based on individual size of pelvis and

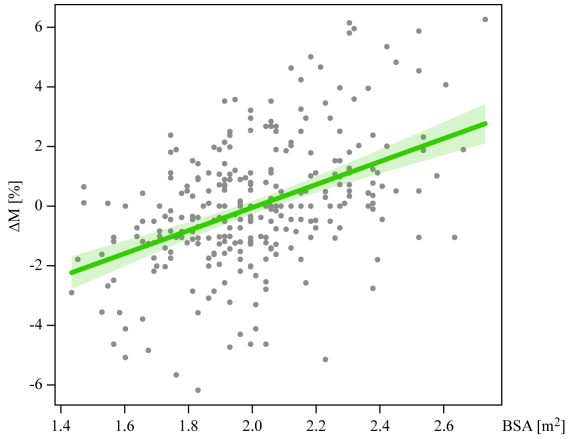

Figure 4.5: The correlation between patients' BSA and change in hip radiographic magnification ΔM.

proximal femur measured by five parameters, (B) isotropic scaling by pelvic width, and (C) isotropic scaling by interhip distance. The relationship between measured geometrical parameters were examined as well.

Anisotropic scaling A yields considerably higher variance in hip joint reaction force than isotropic scaling B or C where the variance in hip joint reactions force is minute (Figure 4.6). Anisotropic scaling A predicts lower average hip load than isotropic scaling B and C that is statistically significant (paired t-test, $p < 0.001$). The peak difference between the hip joint reaction force obtained by anisotropic scaling A and by isotropic scaling B in some patients surpassed $1 \times BW$. Isotropic scaling assumes that bones have mutually proportional dimensions between patients.

Although the hips with larger interhip separation l have significantly ($r = 0.42,\ p = 0.001$) larger iliac height H, no correlation was found between the interhip separation l and the iliac width C ($r = 0.05,\ p = 0.05$) nor lateral coordinate of greater trochanter T_z ($r = -0.01,\ p = 0.05$), Table 4.4.

Table 4.4: Presents reference values, average values, standard deviations and coefficients of correlations r between different geometrical parameters [56]. Statistically significant correlations are marked by * for $p < 0.05$ (treshold $r = 0.1895$), ** for $p < 0.01$ (treshold $r = 0.255$) and *** for $p < 0.001$ (treshold $R = 0.327$), $\alpha = \beta$ in all cases.

Par.	Ref. [mm]	Mean [mm]	StDev [mm]	r				
				l	H	C	T_z	T_y
l	172	201.8	17.7	1.000	0.429^{***}	0.094	0.033	0.296^{**}
H	58	152.4	11.4		1.000	0.295^{**}	0.204^{*}	0.056
C	45	58.8	10.1			1.000	0.311^{**}	-0.189
T_z	51	61.0	7.7				1.000	-0.120
T_y	-23	-10.8	6.2					1.000

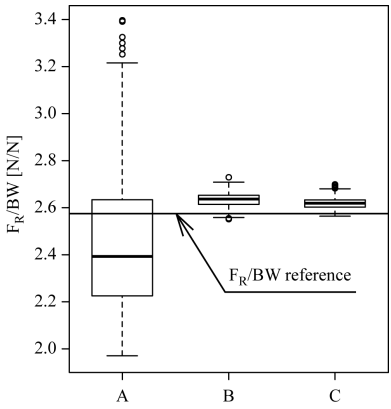

Figure 4.6: Ranges of calculated hip joint reaction force for A – anisotropic scaling, B – isotropic scaling by the pelvic width, C – isotropic scaling by the interhip separation [56].

4.3 Comparison of calculated hip joint reaction force to in vivo measurements

Validation is a major concern for biomechanical models. Only few in-vivo measurements exist for hip joint reaction force, the primary date are provided from measurements using implanted instrumented endoprosthesis [7]. This section was intended to study, if the data predicted by the biomechanical model could be compared to experimental measurements. The hypothesis was tested whether the type

of scaling could improve accuracy of the method.

The influence of type of scaling to the hip joint reaction forces was observed within the study of one patient from HIP98 data. An OpenSim musculoskeletal model was scaled nonuniformly (NS), uniformly by body height (BH) and uniformly by body height, except of pelvis, that was scaled nonuniformly (BHP). A comparison of measured [7] and calculated hip joint reaction forces during normal walking is shown in Figure 4.7. The model predicted the time-course of the hip joint reaction force qualitatively, but it provided considerably higher values then measured. The maximal values of hip joint reaction forces and the relative difference between the calculated forces against the maximal measured force is shown in Table 4.5. The scaling has little effect to the calculated hip joint force.

Table 4.5: Maximum hip joint reaction forces $F_{\max}$ [N]. MD – measured data; NS – nonuniform scaling; BH – uniform scaling (body height); BHP – uniform scaling (body height), nonuniform scaling (pelvis). Difference [%] between experimental data and calculated forces [64, 65].

MD	NS	BH	BHP
2479 N	3313 N	3172 N	3381 N
	33.6 %	27.9 %	36.4 %

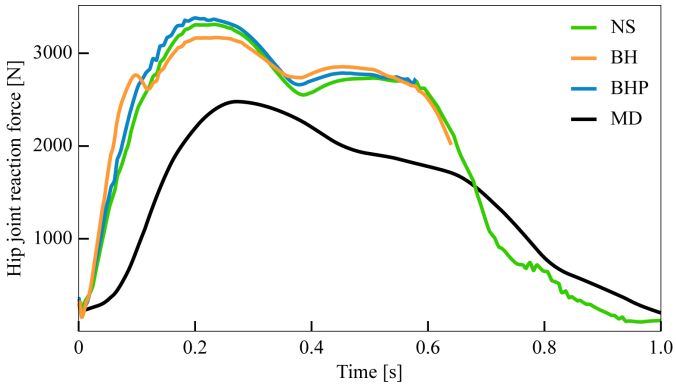

Figure 4.7: Hip joint reaction forces during walk – results from differently scaled models compared with measured data [7]. MD – measured data; NS – nonuniform scaling; BH – uniform scaling (body height); BHP – uniform scaling (body height), nonuniform scaling (pelvis) [64, 65].

4.4 Contribution of musculoskeletal model characteristics to hip muscle and force prediction

Although the muscle attachment points could be scaled to match hip geometry, the scaling of soft tissue parameters is mostly neglected or implemented by simple linear scaling procedure in biomechanical model. Within this study, we would like to examine, how the change in PCSA of individual muscle unit (localized strengthening of single unit of gluteus medius) or in individual muscle group (global strengthening of hip abductors) influences joint and muscle forces predicted by the model.

Localized strengthening of one muscle actuator (glut med 1) overloads this muscle for 29 %, while decreases activity of almost all other hip abductors, Figure 4.8.

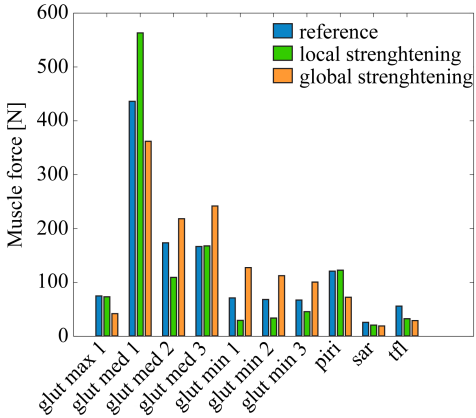

Figure 4.8: Localized strengthening of glut med 1 [55].

4.5 Contact stress calculation

4.5.1 Hip geometry determined by semiautomatic segmentation

Semiautomatic segmentation method for hip cartilage detection was implanted within this study. An example of well detected cartilage

borders represents Figure 4.9. In contrast, an example of semiautomatic segmentation failure is demonstrated in the Figure 4.10.

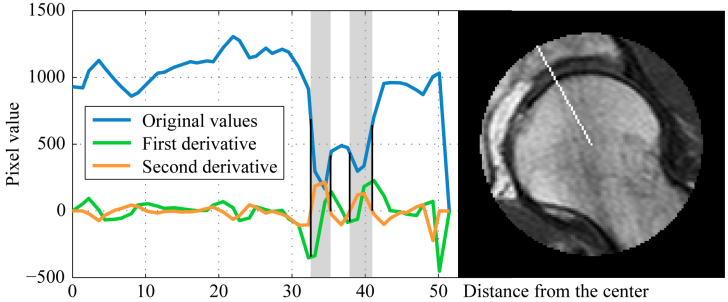

Figure 4.9: Hip joint cartilage segmentation [62]. Example of directional derivatives along radial direction from the center of the circle. The radial line is set off on the image on the right side. The original values of pixels are represented by a blue line, the first derivative by a green line and the second derivative by an orange line [62].

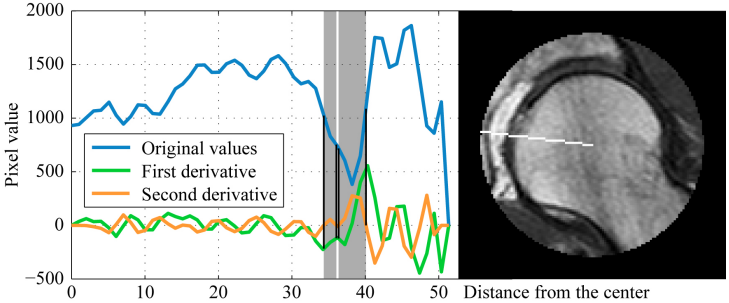

Figure 4.10: Hip joint cartilage segmentation, automated segmentation detects cartilage at anatomically excluded region.

4.5.2 Contact stress model verification

The aim of the model contact stress model verification is to show that computational implementation of the mathematical model and its associated solution is correct. The verification consists of comparison to the benchmark problem of contact between two hemispheres separated by cartilage layer (Section 3.5.3), where analytical solution was derived. The numerical model corresponds well to analytical model, Figure 4.11.

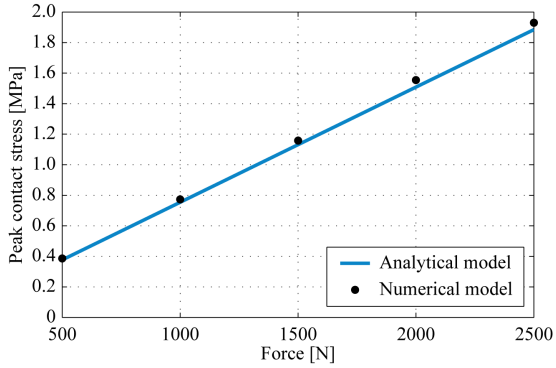

Figure 4.11: Comparison of contact stresses calculated by numerical and analytical model [60, 61].

4.5.3 Effect of patient-specific hip surface on contact stress estimation

The hip joint contact stress distribution is influenced by the loading force, material properties of hip tissues and by geometry of the contact surfaces. The geometry of contact surfaces is mostly simplified to simple spherical shell. This study was intended to test how the individual joint geometry influences contact stress distribution in hip joint. The stress distribution was estimated in static loading position and during walking.

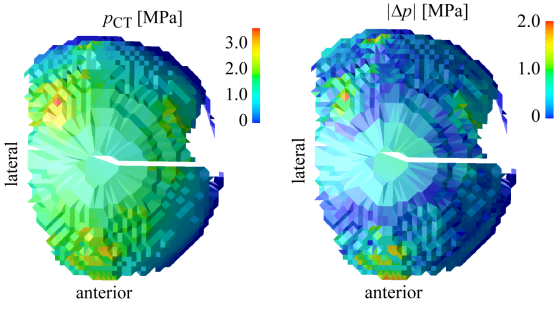

Figure 4.12: Static analysis – one-legged stance [59]. (a) CT model (subject-specific) [60, 61]. (b) Difference $\Delta p = p_{\mathrm{CT}} - p_{\mathrm{radiograph}}$.

In static loading position, the hip loading force $\mathbf{F_R}$ with magnitude 2000 N (2.5 body weight for 80 kg man) lies in the frontal

plane and it is inclined for an angle 5 degrees medially from the vertical axis [28]. Figure 4.12(a) shows projection of hip contact stress to transversal plane, Figure 4.12(b) shows the difference in contact stress distribution between subject-specific model (Figure 4.12(a)) and sphere model based on radiogram. The difference in the peak stress $p_{\max}$, the average contact area A and the mean stress $\overline{p}$ at weight-bearing surface (surface of non-zero contact stress) are given in Table 4.6.

Table 4.6: Contact stresses in the hip joint, static analysis [59].

Parameter		Radiograph	CT
$p_{\max}$	[MPa]	1.7	3.6
$\overline{p}$	[MPa]	0.67	0.77
A	[mm^2]	2784	2274

Although the peak contact stress is greatly influenced by individual geometry, the difference in the mean stress and the contact area are considerably lower. Figure 4.13 presents a distribution of magnitude of differences in contact stress between the radiographic (spherical) model and CT (patient-specific) model weight-bearing area. For given analysis, the stress was evaluated at the center of area of each element in the radiographic model. Most of the elements have error in contact stress estimation lower than 0.5 MPa.

Similar results have been observed when analysing hip joint contact stress distribution during walking. Loading force during one step of walking was taken from Bergmann, et al [7].

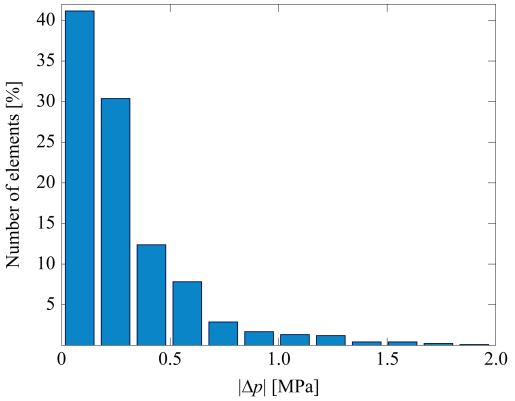

Figure 4.13: Differences in contact stress $|\Delta p|$ [59].

CHAPTER 5

Discussion

5.1 Hip imaging – body measurements for scaling

5.1.1 Influence of workplace

A crucial step in total hip estimating dimensions from radiographs is scaling the template to the magnification of radiograph. The templates are mostly provided prescaled to 20% [4], but the actual magnification is known to vary among patients. The magnification of hip radiograph depends on mutual position of X-ray source, patient and detector plane [25] that might depend on construction of particular X-ray device. This study was intended to estimate, if there is a significant variation of magnification between clinical workplaces.

An external marker at a fixed height over the table was used to ensure repeatability of measurements. Almost constant magnification of the external marker shows that the position of X-ray source, table and detector is identical for all patients [39] as is also required by radiological standards [18]. Lower magnification of external marker observed in present study is a result of placing the marker below the coronal plane of the hip as was also observed by Archibeck et al., 2016 [4]. Certain variation in external marker magnification could be caused by different lateral shift [49].

The magnification of radiographs observed in this study is within range obtained in previous studies. Based on our results (Figure 4.1), we may conclude that differences between studies could also be caused by a difference in radiological magnification among clinical workplaces. The range of observed magnification shows that there are other effects that may influence the radiographic magnification, e.g. distance between the femoral head and the table

(Figure 3.1(a)). These effects could be related to individual body geometry that causes vertical shift [8] or lateral shift of the hip in the projected beam [49].

5.1.2 Influence of obesity

Subcutaneous fat in obese patients increases the distance between the hip joint and the table during pelvis AP projection (Figure 3.1(b)). Therefore, the hip radiograph magnification should be considerably higher in obese patients. The present clinical study of 303 patients after total hip arthroplasty confirmed this assumption.

Similar results have been observed in the previous studies. Archibeck et al., 2016 [4] showed that BMI accounted for a significant amount of variability in the measured magnification both for in internal and external marker. Boese et al., 2015 [8] and The et al., 2007 [50] observed weak correlation between hip radiographic magnification and BMI. Study using a double marker method by King et al., 2009 [30] also showed a weak correlation between BMI and magnification. The weak correlation observed in previous studies, could be explained by factors others than obesity that influence magnification. These effects are shown as data scattering in Figure 4.4 and may be attributed to inter-individual variation between the patients. The data presented within this study are based on cohort taken from homogenous population in the Czech Republic where 95 % of the population are Caucasians. It has been shown that body habitus also depends on race [21] and we may expect a weaker correlation in a non homogenous population. The observed correlation is also affected by the range of studied BMI, e.g. no difference could be found when comparing magnification in normal and overweight patients (Figure 4.2).

The secondary aim of the study was to quantify to what extent obesity affects patient's radiographic magnification. Patients' mass, BMI and BSA are approximately at the same level of significance when predicting hip radiographic magnification (Table 4.3). Calculation of BSA is not straightforward, and discrepancies between the most of the known BSA formulae can reach 0.5 m^2 for normal patient [41]. Therefore we do not recommend using BSA for magnification error estimation.

The clinically tolerable margin of magnification error depends on the steps between implant sizes. Franken et al., 2010 [23] showed,

that to template exactly for a specific implant size, the magnification error should be less than 2 per cent for the ABG-II implant series. Our study shows that the change in radiographic magnification for class-I obese and class-II obese with respect to normal-weight patients is outside the limit proposed by Franken et al., 2010 [23]. The fixed magnification estimation could be improved by considering the patient's BMI. Firstly, the baseline radiographic magnification for normal patients should be estimated at given workplace. Size of the implanted femoral head could be used as the internal marker. The radiographs taken from an archive allows to create a cohort with equivalent representation for both genders. Secondly, 1 per cent should be added for each obesity category to the mean magnification estimated for normal-weight patients. This straightforward method may increase the accuracy of hip pre-operative hip templating, particularly for obese patients.

5.2 Influence of scaling to the reaction force

This study analyses the effects of anisotropic and isotropic scaling methods on calculated hip joint reaction forces subject to patient-specific geometry. Geometrical parameters were obtained from standard AP radiographs while the force was calculated by a three dimensional musculoskeletal model of one-legged stance. It was found that including patient-specific geometry in more detail considerably affects the hip joint reaction force.

The hip joint reaction force computed by using isotropically scaled models (type B and C, Figure 3.2) is nearly insensitive to the changes in input geometrical parameters in one-legged stance. Isotropic scaling modifies the lever arm of the body weight by increasing or decreasing the interhip separation, however, the iliac width and trochanter position are changed in the same proportion [28]. The change in torque of gravitational forces is compensated by the change in muscle moment arms. Therefore, the level of hip joint force in one-legged stance depends on geometry of reference model mostly, if isotropic scaling of both pelvic and femur by the same scaling factor is adopted. As the same reference model was used in all patients, variation in hip joint force is negligible for isotropic scaling.

Isotropic hip scaling (B and C) yields a higher average magnitude of hip joint reaction force than anisotropic scaling A. However, this could be an effect of reference muscle geometry. A reference muscle model derived from the Visible Human Project [3] has lower muscle moment arms than average values of the population considered (Table 4.4) and thus it predicts greater hip force.

As shown in Table 4.4, the overall size of pelvic bone is not directly correlated to the positions of bone prominences serving as muscle attachment points. Hence, scaling based on overall bone size does not accurately predict muscle moment arms and position of the center of rotation as also shown in previous studies [14, 31]. Including the inter-individual variations in pelvic and proximal femur dimensions in anisotropic scaling increases range of predicted hip joint force significantly.

5.3 Validation of calculated hip joint reaction force to in vivo measurements

Within this study, a generic muscle model of the lower leg provided as a part of the OpenSim software package was compared to data obtained from implanted instrumented endoprosthesis.

Our results indicate that the mathematical model gives considerably higher hip joint forces than ones obtained from experimental measurements. Several factors could be identified that influence accuracy of measured method: from improper kinematics a kinetics imported into mechanical model to musculoskeletal model geometry and functional characteristics. The first source of error could be improper kinematics imported into model caused by inaccurate marker positions defined in OpenSim and HIP98 data. It has been shown, that change in kinematic affects the hip joint load considerably [12, 53].

The second reason for hip joint force overestimation predicted by mathematical model has been may be oversimplified geometry of the musculoskeletal model adopted in the OpenSim generic model. The model included 92 muscle actuators only. The muscle actuators may not be suitable to generate desired moments [35]. By increasing the number of the muscles, the muscle force would be decreased as more muscles will have favourable moment arms. This was shown by Modenese et al., 2011 who used a muscle model with 38 muscles

divided in 163 actuators. By adopting more accurate joint gemetry, the average relative variability of the experimental hip joint reaction force derived from HIP98 data does not exceed 8 % for both level walking and stair climbing [36].

5.4 Contribution of musculoskeletal model characteristics to hip muscle and force prediction

Within the present study, muscle-actuated dynamic simulations was used to determine how individual muscle strength influences the muscle forces distribution during gait. Musculoskeletal simulation was adopted because it provides controlled environment elucidating cause and effect relationship and also because important variables, such as muscle forces, are generally not measurable [44].

Strengthening of individual muscle unit increases its load bearing considerably. Strengthened muscle becomes overloaded while the activity of other abductors is decreased in comparison to reference state. Local muscle strengthening could be dangerous for hip stability as the underloaded muscles may atrophy while the overloaded muscle hypertrophy and hip imbalance may develop.

Presented study indicates that complex strengthening is more favourable. This statement, well established empirically, has important biomechanical consequences. It is shown that the global strengthening distributes force between more muscle and it dynamically stabilizes the hip. It was shown, that muscle fatigue is related to mechanical stress in muscles [15]. Redistribution of muscle force between the muscles decreases the mechanical stress and thus improves muscle performance [27]. For this model the average relative variability of the experimental hip joint reaction force resultant derived from HIP98 data does not exceed 8 % for both level walking and stair climbing [36].

5.5 Contact stress calculation

The first step in calculation of the patient-specific stress is the evaluation of hip geometry. Within this study, an algorithm for semi-automatic segmentation of articular cartilage was developed and

tested. Two-dimensional segmentation proved to be stable for most of the cartilage regions and three-dimensional cartilage model could be created using described method. This approach is applicable to both MRI and CT images.

It was shown in Figure 4.12(a) that the mathematical simulation may provide a nonuniform and nonsymmetrical contact stress distribution if inhomogeneities in the cartilage geometry are considered. The stress distribution varies slowly over the most of the load-bearing surface while singular stress peaks can reach more than twice the value of stress obtained at the majority of the load-bearing surface. The reason, why the experiments did not show the uniform stress distribution in addition to the stress peaks could be a limited range of the pressure sensors, especially in the measurements using the pressure sensitive film that provides the spatial contact stress analysis [6]. For example, Sparks et al., 2005 [47] measured the hip contact stress with the pressure sensitive film adjusted to the pressure in the range of 2.4-9.6 MPa. These measurements cannot reveal the overall stress distribution because the corresponding values of stress would be below the sensitivity of the pressure film and the film can measure only the stress peaks. The more accurate instrumented hemiarthroplasty [11] or in vitro pressure transducers [9] give the values of the contact stress at particular points of the articular surface with a limited spatial resolution. However, these measurements show that the regions of high stress are relatively small [37] and that stress at the rest of the articular surface is rather low which is in accordance with our simulations.

However, also other results confirm the main conclusion of the study, that the mathematical model assuming uniform cartilage thickness may provide a realistic assessment of the hip contact stress distribution. For example, if the stress 5 MPa frequently measured experimetally will be acting in the whole load-bearing area, the cartilage deformations will be 50 % according to Eq. 3.5. However, the measurements of the cartilage deformation in a cadaver hip showed changes in cartilage thickness on the order of 10 % and 20 % under load 1.2 and 2.5 BW, respectively [5]. Taking into account mechanical properties of the cartilage [46, 45], the measured deformation roughly corresponds to the contact stress 2 MPa, the same stress level as the value of stress at the stress pole (p_0).

CHAPTER 6

Conclusion

The application of simple generic biomechanical models for prediction of patient-specific hip joint loading is questionable. Therefore, influence of several simplifying assumptions to the results from musculoskeletal models was evaluated within this study. We compared the effect of generic and patient-specific inputs to the predicted biomechanical status of the hip. Namely, we have studied the accuracy of geometrical parameters measured from plane radiographs, the effect of musculoskeletal model geometry and muscle units properties to the hip joint force and contact stress prediction, and validation against experimental data.

Within clinical study was determined that both the workplace and obesity influence hip radiographic magnification. Our study supplements previous studies by showing that magnification of hip radiographs depends not only on marker and patient-specific factors, but also on clinical workplace. It indicates potential limits in generalizability of results of studies dealing with preoperative planning accuracy to other institutions [66, 57]. We may conclude that quantitative results on hip radiographic magnification for templating, such as optimal value of fixed magnification, cannot be simply transferred from one workplace to another [66, 57].

This study futher shows that obese patients have significantly greater magnification of hip digital radiographs and it should be considered during hip templating. If the magnification marker method is not applicable, BMI could be used to estimate the increase in hip radiographic magnification due to obesity. Based on our results we recommend that 1 per cent is added to the radiographic magnification estimated for normal-weight patients for each subsequent BMI obesity [67, 58]. To account for gender difference, the 0.7 % and 1.2 % for male and female is added, respectively [67, 58].

To effect of isotropic and anisotropic scaling on the hip joint reaction force was assessed in the clinical study. It was shown that

scaling based on gross bone dimension (isotropic scaling) does not scale muscle moment arms accurately and does not predict hip load accurately. Hip joint force estimated by isotropic scaling depends mostly on reference musculoskeletal geometry. To improve estimation of the hip joint reaction force in an individual, determination of more hip and pelvic geometrical parameters should be included in the scaling method (anisotropic scaling) [56]. The difference between isotropic and anisotropic scaling may be as high as patient's body weight[56].

The hip joint reaction force was predicted by musculoskeletal model [54] and compared to experimental data to provide model validation. Our results shows that the calculated hip joint reaction force is qualitatively comparable with experimental data. However, the magnitude of hip joint reaction force was overestimated by roughly 30 percent [64, 65]. This is likely to be caused by insufficient number of muscles in the model or inaccurate scaling of patient-specific geometry and thus obtaining of smaller moment arms of muscles.

We have also obtained that musculoskeletal model characteristics (maximal isometric muscle force) influence the hip muscle force distribution but the hip joint reaction force prediction [55]. The strengthening of individual muscle overloads this muscle and causes muscle imbalance.

Contact stress distribution in the hip joint was assessed by mathematical model [60, 61]. Patient-specific hip contact model was created from CT and MRI data. This study shows that geometrically simplified and patient-specific models are comparable in overall stress distribution but patient-specific model predicts much higher value of peak contact stress [59].

We may conclude that assumptions used in generic biomechanical models influence their results in patient-specific studies considerably. The prediction of biomechanical parameters could be improved, if the geometry and properties of the model are adopted for given patient properly. This study indicates potential limits that should be considered when generic models are used in the clinical practice.

Bibliography

[1] *delaunay*, aug 2009. Available at `http://www.mathworks.com/access/helpdesk/help/techdoc/ref/delaunay.html`.

[2] *fsolve*, jan 2017. Available at `https://www.mathworks.com/help/optim/ug/fsolve.html?BB=1`.

[3] M. J. Ackerman. Accessing the visible human project. *D-Lib Magazine*, 1(4), oct 1995.

[4] M. J. Archibeck, T. Cummins, K. R. Tripuraneni, J. T. Carothers, C. Murray-Krezan, M. Hattab, and R. E. White. Inaccuracies in the use of magnification markers in digital hip radiographs. *Clinical Orthopaedics and Related Research®*, 474(8):1812–1817, jan 2016.

[5] G. A. Ateshian and C. T. Hung. *Functional tissue engineering*, chapter Functional, pages 46–68. Springer-Verlag, New York, 2003.

[6] B. K. Bay, A. J. Hamel, S. A. Olson, and N. A. Sharkey. Statically equivalent load and support conditions produce different hip joint contact pressures and periacetabular strains. *Journal of Biomechanics*, 30(2):193–196, feb 1997.

[7] G. Bergmann, G. Deuretzbacher, M. Heller, F. Graichen, A. Rohlmann, J. Strauss, and G. Duda. Hip contact forces and gait patterns from routine activities. *Journal of Biomechanics*, 34(7):859–871, jul 2001.

[8] C. K. Boese, P. Lechler, L. Rose, J. Dargel, J. Oppermann, P. Eysel, H. Geiges, and J. Bredow. Calibration markers for digital templating in total hip arthroplasty. *PLOS ONE*, 10(7):e0128529, jul 2015.

[9] T. D. Brown and D. T. Shaw. In vitro contact stress distributions in the natural human hip. *Journal of Biomechanics*, 16(6):373–384, jan 1983.

[10] M. Cadova, M. Vilimek, and M. Daniel. A comparative study of muscle force estimates using Huxley's and Hill's muscle model. *Comput. Methods Biomech. Biomed. Engin.*, 17(4):1–7, may 2012.

[11] C. E. Carlson, R. W. Mann, and W. H. Harris. A radio telemetry device for monitoring cartilage surface pressures in the human hip. *IEEE Transactions on Biomedical Engineering*, BME-21(4):257–264, jul 1974.

[12] A. Carriero, A. Zavatsky, J. Stebbins, T. Theologis, G. Lenaerts, I. Jonkers, and S. J. Shefelbine. Influence of altered gait patterns on the hip joint contact forces. *Computer Methods in Biomechanics and Biomedical Engineering*, 17(4):352–359, 2012. Epub 2012 May 16.

[13] D. R. Carter and G. S. Beaupré. Correspondence. *Journal of Biomechanics*, 32(11):1255 – 1256, 1999.

[14] T. A. Correa, R. Baker, H. K. Graham, and M. G. Pandy. Accuracy of generic musculoskeletal models in predicting the functional roles of muscles in human gait. *Journal of Biomechanics*, 44(11):2096–2105, jul 2011.

[15] R. D. Crowninshield and R. A. Brand. A physiologically based criterion of muscle force prediction in locomotion. *Journal of Biomechanics*, 14(11):793–801, jan 1981.

[16] R. D. Crowninshield, R. C. Johnston, J. G. Andrews, and R. A. Brand. A biomechanical investigation of the human hip. *Journal of Biomechanics*, 11(1-2):75–85, jan 1978.

[17] G. Daubes. Variations in human stature. *Popular Science Monthly. D. Appleton and Company, New York*, page 31, 1887.

[18] A. M. Davies, K. J. Johnson, and R. W. Whitehouse, editors. *Imaging of the Hip & Bony Pelvis. Medical Radiology.* Springer Berlin Heidelberg, 2006.

[19] S. L. Delp, F. C. Anderson, A. S. Arnold, P. Loan, A. Habib, C. T. John, E. Guendelman, and D. G. Thelen. OpenSim: Open-source software to create and analyze dynamic simulations of movement. *IEEE Transactions on Biomedical Engineering*, 54(11):1940–1950, nov 2007.

[20] S. L. Delp, J. Loan, M. Hoy, F. Zajac, E. Topp, and J. Rosen. An interactive graphics-based model of the lower extremity to study orthopaedic surgical procedures. *IEEE Transactions on Biomedical Engineering*, 37(8):757–767, 1990.

[21] E. W. Demerath, S. S. Sun, N. Rogers, M. Lee, D. Reed, A. C. Choh, W. Couch, S. A. Czerwinski, W. C. Chumlea, R. M. Siervogel, and B. Towne. Anatomical patterning of visceral adipose tissue: Race, sex, and age variation. *Obesity*, 15(12):2984–2993, dec 2007.

[22] M. L. Drumm, A. G. Ziady, and P. B. Davis. Genetic variation and clinical heterogeneity in cystic fibrosis. *Annual Review of Pathology: Mechanisms of Disease*, 7(1):267–282, feb 2012.

[23] M. Franken, B. Grimm, and I. Heyligers. A comparison of four systems for calibration when templating for total hip replacement with digital radiography. *Journal of Bone and Joint Surgery - British Volume*, 92-B(1):136–141, jan 2010.

[24] B. J. Fregly. Design of optimal treatments for neuromusculoskeletal disorders using patient-specific multibody dynamic models. *International journal for computational vision and biomechnanics*, 2(2):145–155, jul 2009.

[25] G. Heinert, J. Hendricks, and M. D. Loeffler. Digital templating in hip replacement with and without radiological markers. *Journal of Bone and Joint Surgery - British Volume*, 91-B(4):459–462, apr 2009.

[26] J. Higginson, F. Zajac, R. Neptune, S. Kautz, and S. Delp. Muscle contributions to support during gait in an individual with post-stroke hemiparesis. *Journal of Biomechanics*, 39(10):1769–1777, jan 2006.

[27] M. K. Horsman, H. Koopman, F. van der Helm, L. P. Prosé, and H. Veeger. Morphological muscle and joint parameters

for musculoskeletal modelling of the lower extremity. *Clinical Biomechanics*, 22(2):239–247, feb 2007.

[28] A. Iglič, V. Kralj-Iglič, M. Daniel, and A. Maček-Lebar. Computer determination of contact stress distribution and size of weight bearing area in the human hip joint. *Computer Methods in Biomechanics and Biomedical Engineering*, 5(2):185–192, jan 2002.

[29] H. Kainz, C. P. Carty, S. Maine, H. P. Walsh, D. G. Lloyd, and L. Modenese. Effects of hip joint centre mislocation on gait kinematics of children with cerebral palsy calculated using patient-specific direct and inverse kinematic models. *Gait & Posture*, jun 2017.

[30] R. J. King, P. Makrides, J. A. Gill, S. Karthikeyan, S. J. Krikler, and D. R. Griffin. A novel method of accurately calculating the radiological magnification of the hip. *Journal of Bone and Joint Surgery - British Volume*, 91-B(9):1217–1222, aug 2009.

[31] G. Lenaerts, W. Bartels, F. Gelaude, M. Mulier, A. Spaepen, G. V. der Perre, and I. Jonkers. Subject-specific hip geometry and hip joint centre location affects calculated contact forces at the hip during gait. *Journal of Biomechanics*, 42(9):1246–1251, jun 2009.

[32] E. Livingston and S. Lee. Body surface area prediction in normal-weight and obese patients. *American Journal of Physiology–Endocrinology and Metabolism*, 281(3):E586–E591, 2001.

[33] K. Manal and T. S. Buchanan. Subject-specific estimates of tendon slack length: A numerical method. *Journal of Applied Biomechanics*, 20(2):195–203, may 2004.

[34] MATLAB. *version 7.9.0 (R2009b)*. The MathWorks Inc., Natick, Massachusetts, 2009.

[35] L. Modenese, A. Gopalakrishnan, and A. Phillips. Application of a falsification strategy to a musculoskeletal model of the lower limb and accuracy of the predicted hip contact force vector. *Journal of Biomechanics*, 46(6):1193–1200, apr 2013.

[36] L. Modenese, A. Phillips, and A. Bull. An open source lower limb model: Hip joint validation. *J. Biomech.*, 44(12):2185–2193, aug 2011.

[37] K. C. Morrell, W. A. Hodge, D. E. Krebs, and R. W. Mann. Corroboration of in vivo cartilage pressures with implications for synovial joint tribology and osteoarthritis causation. *Proceedings of the National Academy of Sciences*, 102(41):14819–14824, oct 2005.

[38] M. L. Neal and R. Kerckhoffs. Current progress in patient-specific modeling. *Briefings in Bioinformatics*, 11(1):111–126, dec 2009.

[39] W. H. Organization. *Obesity: preventing and managing the global epidemic. Report of a WHO consultation.* 894: i–xii. World Health Organ. Tech. Rep. Ser., 2000. ISSN 0512-3054. ISBN 92 4 120894 5.

[40] C. Paul, M. Bellotti, S. Jezernik, and A. Curt. Development of a human neuro-musculo-skeletal model for investigation of spinal cord injury. *Biological Cybernetics*, 93(3):153–170, aug 2005.

[41] G. Redlarski, A. Palkowski, and M. Krawczuk. Body surface area formulae: an alarming ambiguity. *Scientific Reports*, 6:27966, jun 2016.

[42] J. A. Reinbolt, M. D. Fox, M. H. Schwartz, and S. L. Delp. Predicting outcomes of rectus femoris transfer surgery. *Gait & Posture*, 30(1):100–105, jul 2009.

[43] P. Samuel. *Computing constrained Delaunay triangulations*, aug 2009. Available at `http://www.geom.uiuc.edu/~samuelp/del_project.html`.

[44] A. Seth, M. Sherman, J. A. Reinbolt, and S. L. Delp. OpenSim: a musculoskeletal modeling and simulation framework for in silico investigations and exchange. *Procedia IUTAM*, 2:212–232, 2011.

[45] D. E. Shepherd and B. B. Seedhom. The 'instantaneous' compressive modulus of human articular cartilage in joints of the lower limb. *Rheumatology*, 38(2):124, 1999.

[46] D. E. Shepherd and B. B. Seedhom. Thickness of human articular cartilage in joints of the lower limb. *Annals of the Rheumatic Diseases*, 58(1):27–34, jan 1999.

[47] D. R. Sparks, D. P. Beason, B. S. Etheridge, J. E. Alonso, and A. W. Eberhardt. Contact pressures in the flexed hip joint during lateral trochanteric loading. *Journal of Orthopaedic Research*, 23(2):359–366, mar 2005.

[48] D. Tahmoush and J. Silvious. Gait variations in human micro-doppler. *International Journal of Electronics and Telecommunications*, 57(1), jan 2011.

[49] B. The, R. L. Diercks, R. E. Stewart, P. M. A. van Ooijen, and J. R. van Horn. Digital correction of magnification in pelvic x rays for preoperative planning of hip joint replacements: Theoretical development and clinical results of a new protocol. *Medical Physics*, 32(8):2580–2589, jul 2005.

[50] B. The, J. W. J. Kootstra, A. H. Hosman, N. Verdonschot, C. L. E. Gerritsma, and R. L. Diercks. Comparison of techniques for correction of magnification of pelvic x-rays for hip surgery planning. *Journal of Digital Imaging*, 20(4):329–335, dec 2007.

[51] D. van Geemen, P. W. R. Vis, S. Soekhradj-Soechit, J. P. Sluijter, M. de Liefde-van Beest, J. Kluin, and C. V. Bouten. Decreased mechanical properties of heart valve tissue constructs cultured in platelet lysate as compared to fetal bovine serum. *Tissue Engineering Part C: Methods*, 17(5):607–617, may 2011.

[52] L. Q. Wan, C. Miller, X. E. Guo, and V. C. Mow. Fixed electrical charges and mobile ions affect the measurable mechano-electrochemical properties of charged-hydrated biological tissues: the articular cartilage paradigm. *Mech Chem Biosyst*, 1(1):81–99, mar 2004.

[53] M. Wesseling, L. C. Derikx, F. de Groote, W. Bartels, C. Meyer, N. Verdonschot, and I. Jonkers. Muscle optimization techniques impact the magnitude of calculated hip joint contact forces. *Journal of Orthopaedic Research*, 33(3):430–438, mar 2015. Epub 2014 Dec 9.

List of publications related to the dissertation thesis

Articles

[54] M. Daniel, M. Tomanová, J. Hornová, I. Novotná, L. Lhotská. Biomechanical analysis of INFINITY rehabilitation method for treatment of low back pain. *Journal of Physical Therapy Science*, 29(5):832–838, 2017. (Scopus Cite Score 1.53)

[55] M. Daniel, J. Hornová, K. Doubrava, M. Tomanová. Biomechanical analysis of local and global strengthening of gluteus medius. *The Turkish Journal of Physical Medicine and Rehabilitation*, 63(3), 2017. (IF 0.186)

[56] J. Hornová, A. Iglič, V. Kralj-Iglič, D. R. Pedersen, M. Daniel. Effect of patient-specific model scaling on hip joint reaction force in one-legged stance – study of 356 hips. *Acta of Bioengineering and Biomechanics*, 2017. Accepted for publication. (IF 0.914)

[57] J. Hornová, R. Růžička, M. Hrubina, E. Šťastmý, A. Košková, P. Fulín, J. Gallo, M. Daniel. Magnification of digital hip radiographs differs between clinical workplaces. 2017. Submitted to Plos One.

[58] J. Hornová, R. Růžička, M. Hrubina, E. Šťastmý, A. Košková, P. Fulín, J. Gallo, M. Daniel. Magnification of hip radiographs for obese patients: recommendation for preoperative templating. 2017. Submitted to International Orthopaedics.

Conference proceedings

[59] M. Daniel, J. Hornová, A. Iglič. Peak contact stress in human hip joint – biomechanics or mechanobiology? In *34th Annual Meeting of the American Society of Biomechanics*, pages 392–393, Stanford, US, 2010.

[60] J. Hornová, M. Daniel. Determination of hip joint contact pressure from CT or MR images. In *Human Biomechanics 2010*, pages 115–120, Liberec, CZ, 2010.

[61] J. Hornová, M. Daniel. La détermination de la pression contacte dans la hanche des images de TDM et RMN. In *Studentská tvůrčí činnost 2010*, pages 1–15, Praha, CZ, 2010.

[62] J. Hornová, M. Daniel. Semiautomatic segmentation of the hip joint cartilage from MR images. In *Workshop On Applied Mechanics WAM 2011*, pages 11–12, Praha, CZ, 2011.

[63] M. Daniel, J. Hornová, A. Iglič, V. Kralj-Iglič. Effect of patient-specific model scaling on hip joint reaction force in one-legged stance study of 368 hips. In *14th Conference on Human Biomechanics*, pages 6–7, Praha, CZ, 2012.

[64] J. Hornová, M. Daniel. Comparison of calculated hip joint reaction forces with experimental data. In *16th Workshop of Applied Mechanics*, pages 11, Praha, CZ, 2012.

[65] J. Hornová, M. Daniel. Hjp joint reaction forceestimated using OpenSim - comparison to measured data. *Proceedings of the 19th Congress of the European Society of Biomechanics*, Patras, 2013.

[66] J. Hornová, R. Růžička, M. Hrubina, E. Šťastmý, A. Košková, P. Fulín, J. Gallo, M. Daniel. Influence of the choice of radiographic workplace on the radiographic magnification. In *22nd Workshop of Applied Mechanics – Book of Papers*, pages 20–24, Praha, CZ, 2017.

[67] J. Hornová, R. Růžička, M. Hrubina, E. Šťastmý, A. Košková, P. Fulín, J. Gallo, M. Daniel. Grater radiographic magnification of obese patients. *22nd Workshop of Applied Mechanics – Book of Papers*, pages 25–31, Praha, CZ, 2017.